Volume 1 No. 2, June 2011
International Journal of Information and Communication Technology Research

http://www.esjournals.org

Recent Progress of $LiNbO_3$ Based Electrooptic Modulators with Non Return to Zero (NRZ) Coding in High Speed Photonic Networks

Abd El–Naser A. Mohamed, Mohamed A. Metawe'e
Ahmed Nabih Zaki Rashed*, Amira M. Bendary
Electronics and Electrical Communications Engineering Department
Faculty of Electronic Engineering, Menouf 32951, Menoufia University, EGYPT
* ahmed_733@yahoo.com

ABSTRACT

High frequency and broad bandwidth technology development in photonic network applications is being driven by the need to quickly process and distribute large amounts of information. Due to the high cost, complexity, and performance limitations of electronic high frequency systems, hybrid electrical-optical or all-optical systems are necessary. Current off-theshelf optical components function well at frequencies below 20 GHz, but their performance begins to degrade quickly above 40 GHz. This performance degradation results primarily from limitations in the crystalline electrooptic materials currently used to fabricate optical components. Optical components and integrated optical devices that operate at high frequency and with high bandwidth are necessary for next generation applications such as high capacity optical networks, high speed microprocessors, and high frequency wireless communications. Therefore, this paper has proposed the recent progress of LiNbO3 based Electrooptic modulator devices in high speed photonic access communication networks. We have investigated the cut-off frequency, 3-dB bandwidth, modulation bandwidth, transmission bit rates and products within NRZ coding over wide range of the affecting parameters.

Keywords: *Integrated optoelectronics, Optoelectronic devices, Optical modulation, Optical planar waveguide, and NRZ coding.*

I. INTRODUCTION

The ferroelectric material lithium niobate ($LiNbO_3$) has been extensively applied to optical devices. It has excellent electro-optic and optical properties that is [1], it has a large electro-optic effect and is capable of a high-speed response. It is also transparent for infrared light and it is easy to fabricate into low-loss channel waveguides by diffusing titanium. Consequently, various high-performance optical waveguided $LiNbO_3$ devices have been developed for the terminal functions of external intensity modulators, phase modulators, and multi/demultiplexers, as well as switch arrays for optical fiber network systems. In particular, these $LiNbO_3$ devices are very useful for optical wavelength division multiplexing (WDM) systems because of the possibility of operation in the range of wide-wavelength infrared light with a single device due to its transparence [2]. LiNbO3 external modulators have been developed for extensive use in high speed and long-distance optical fiber transmission systems. This is because they can offer the advantages of modulation exceeding 10 Gbits/sec combined with a low driving voltage, and they can eliminate the dynamic laser wavelength chirping which limits the span-rate system product due to their fiber dispersion characteristics. $LiNbO_3$ external modulators can also offer pure phase modulation in coherent systems and can realize various optical signal processors. As the bit rate of optical network systems becomes higher [3], it becomes more difficult to drive a modulator with a high voltage due to the restrictions of electrical instruments, in particular, electrical driving amplifiers. Therefore, reduction of the driving voltage of an $LiNbO_3$ modulator with a broadband characteristic is an extremely important issue for realizing future high-speed optical transmission systems [4].

Present communication technology relies on fiber-optic systems which include light sources such as a laser, optical fiber [5], integrated optical components such as modulators and switches, and optical detectors. The lasers and detectors are fabricated using semiconductor materials, and the integrated optical components are generally fabricated using electrooptic single crystal materials such as $LiNbO_3$. Among the integrated optical components, the contribution from electrooptic modulators using $LiNbO_3$ waveguide structures has been significant in the last several decades due to their high-speed and chirp-free nature. The essential requirements for efficient electrooptic modulation are low half-wave (switching) voltage and broad 3-dB modulation bandwidth. Fast Mach-Zehnder $LiNbO_3$ modulators with low operating voltage fabricated in electrooptic modulator technology have the potential to considerably cut costs for high speed optical transceivers. So far, the fastest broadband light modulation in silicon technology was achieved with free-carrier injection, which allowed modulation up to 30 GHz [6]. On the other hand, much higher modulation frequencies can be achieved with polymer based material systems through the virtually instantaneous electro-optic effect [7].

In the present work, we have taken in to account one of the most important components of a nanophotonic communication system is a fast electrooptic modulator, which takes in a direct current optical input signal and switches it on/off using a high data rate electronic signal. Modulation is achieved by inducing a change in the phase

or the intensity of the light, using a refractive index change or an absorption change, respectively. Moreover we have analyzed parametrically the transmission data rate, operating signal bandwidth, modulation bandwidth, device performance index, and transmission data rate length product within NRZ coding as a good criteria for high speed electrooptic device performance and efficiency.

II. DIFFERENT MODULATION SCHEMES WITH ELECTROOPTIC NODULATOR DEVICES

Figure 1 show single-mode channel waveguided device structures using z-cut $LiNbO_3$ crystals, where a low-refractive-index buffer layer of SiO_2 film is formed between the electrode and the $LiNbO_3$ substrate to prevent light absorption by the metal. For external modulators, the absence of optical wavelength chirping in modulated signals is essential in high-speed and long-distance optical transmission systems. A Mach-Zehnder interferometric modulator has an ideal zero chirp [8] with push-pull operation , i.e., an increase in the refractive index of one waveguide causes a corresponding decrease in that of the other. Consequently, a Mach-Zehnder interferometer is normally utilized for high-speed intensity modulators, whereas a directional coupler is used for integrated switching devices [9].

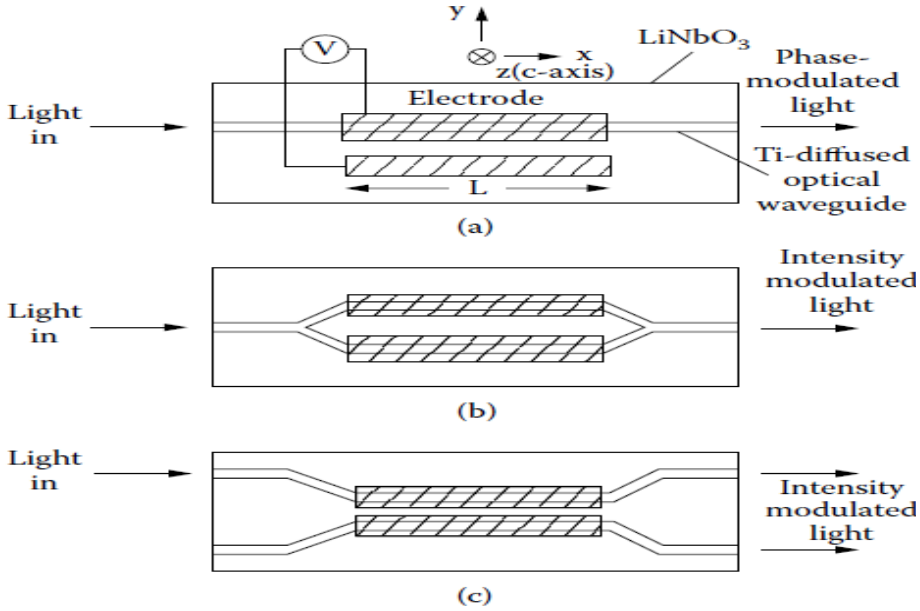

Fig. 1: Scheme of typical waveguided z-cut $LiNbO_3$ devices. (a) phase modulator, (b) intensity modulator using Mach-Zehnder interferometer, and (c) intensity modulator using directional coupler.

III. DEVICE MODELING ANALYSIS

To use the highest electrooptic coefficient in $LiNbO_3$ (r_{33}), the externally applied electric field should be parallel to the Z-axis [7]. Therefore, in order to optimize the interaction between the electric field and the optical mode [8], in a Z-cut wafer the electrodes should be positioned on top of the waveguide arms, while in an X-cut wafer the electrodes should be located on both sides of the branches. In these conditions the extraordinary refractive index change by electro-optic effect in $LiNbO_3$ is given by [9]:

$$\Delta n_e = 0.5\, n_e\, r_{33}\, E_z \ , \qquad (1)$$

Where n_e is the effective refractive index of the material based electrooptic modulator device, r_{33} is the corresponding electrooptic coefficient in pm/Volt, E_z is the applied electic field in Z-direction in Volt/cm. The integrated Mach-Zehnder intensity modulator is perhaps the paradigm of integrated optical devices, and it has been successfully used in optics communications technology. The theoretical value for the half-wave voltage of the integrated electro-optic modulator or switching voltage can be calculated using the expression [10]:

$$V_\pi = \frac{\lambda\, g}{L_m\, n_e^3\, r_{33}\, \Gamma} \ , \qquad (2)$$

Where λ is the operating signal wavelength in μm, g is the gap between electrodes in μm, L_m is the modulator length in cm, and Γ is confinement factor (factor with relates the overlap between the applied electric field and the propagating modal field). The transmittance of an optical signal through the modulator using the following equation:

$$T_m = e^{-\alpha L_m} \quad , \text{dB} \tag{3}$$

Where α is the power absorption coefficient in dB/cm. The resistance of modulator device can be measured by estimating the device dimensions as the following equation:

$$R = \rho \frac{L_m}{wd} \quad , \tag{4}$$

Where ρ is the resistivity, d is the modulator thickness, and w is the modulator width. The time constant, τ of the modulator device can be calculated as follows [9]:

$$\tau = RC \ , \tag{5}$$

The cut-off frequency, $f_{cut\text{-}off}$ of the modulator device is calculated from the RC time constant as the following:

$$f_{cut-off} = \frac{1}{2\pi RC} \ , \tag{6}$$

The relative refractive index change induces an optical phase modulation of:

$$\Delta\phi = k_0 L_m \Delta n_e \quad , \tag{7}$$

Where $k_0=2\pi/\lambda$ is the wave number. The electrical 3-dB bandwidth $f_{3\text{-dB}}$ for which modulation voltage, V_m is reduced by $(1/\sqrt{2})$ from its value can be expressed as [10]:

$$f_{3-dB} = \frac{1}{\pi R \varepsilon_{eff} C L_m} \ , \tag{8}$$

Where C is the capacitance in pf, ε_{eff} is the effective RF relative dielectric constant. The bandwidth is reduced by the electrooptic device loss. Under the perfect velocity matching condition [11], achievable modulation bandwidth f_m is:

$$f_m = \frac{6.84}{\alpha L_m} \ , \text{GHz} \tag{9}$$

For $LiNbO_3$ material, the investigation of both the thermal and spectral variations of the effective waveguide refractive index (n_e) require empirical equation. The set of parameters required to completely characterize the temperature dependence of the refractive-index is given below, Sellmeier equation is under the form [12]:

$$n_e = \sqrt{A_1 + A_2 H + \frac{A_3 + A_4 H}{\lambda^2 - (A_5 + A_6 H)^2} + \frac{A_7 + A_8 H}{\lambda^2 - A_9^2} - A_{10}\lambda} \ , \tag{10}$$

Where λ is the optical signal wavelength in μm and $H = T^2 - T_0^2$, T is the ambient temperature in K, and T_0 is the room temperature (300 K). The set of parameters of equation coefficients ($LiNbO_3$) are recast and dimensionally adjusted as: A_1=5.35583, A_2=4.629x10^{-7}, A_3=0.100473, A_4=3.862x10^{-8}, A_5=0.20692, A_6=-0.89x10^{-8}, A_7=100, A_8=2.657 x10^{-5}, A_9=11.34927, and A_{10}=0.01533. Equation (10) can be simplified as the following:

$$n_e = \sqrt{A_{12} + \frac{A_{34}}{\lambda^2 - A_{56}^2} + \frac{A_{78}}{\lambda^2 - A_9^2} - A_{10}\lambda} \ , \tag{11}$$

Where: $A_{12}=A_1+A_2H$, $A_{34}=A_3+A_4H$, $A_{56}=A_5+A_6H$, and $A_{78}=A_7+A_8H$. Then the first and second differentiation of Eq. (11) with respect to operating signal wavelength λ which gives:

$$\frac{dn_e}{d\lambda} = \left(\frac{-\lambda}{n_e}\right) \cdot \left(\frac{A_{34}}{\left(\lambda^2 - A_{56}^2\right)^2} + \frac{A_{78}}{\left(\lambda^2 - A_9^2\right)^2} - A_{10} \right) \ , \tag{12}$$

$$\frac{d^2 n_e}{d\lambda^2} = \left(\frac{1}{n_e}\right) \cdot \left(\frac{A_{34}\left(2 - \left(\lambda^2 - A_{56}^2\right)\right)}{\left(\lambda^2 - A_{56}^2\right)^2} + \frac{A_{78}\left(2 - \left(\lambda^2 - A_9^2\right)\right)}{\left(\lambda^2 - A_9^2\right)^2} + A_{10} \right) \ , \tag{13}$$

The material dispersion based electrooptic modulator, $D_{mat.}$ which is given by the following equation [13]:

$$D_{mat.} = -\left(\frac{L_m . \Delta\lambda . \lambda}{c}\right) \cdot \left(\frac{d^2 n_e}{d\lambda^2}\right) \ , \tag{14}$$

The modal-dispersion delay, D_{modal} for a multi mode step-index electrooptic device with length L_m, is given by:

$$D_{\mathrm{mod}\,al} = L_m n_e \Delta n_e / c \quad , \tag{15}$$

Where the total dispersion coefficient [15], $D_t=D_{mat.}+D_{modal}$. In addition to providing sufficient power to the receiver, the system must also satisfy the bandwidth requirements imposed by the rate at which data are transmitted. A convenient method of accounting for the bandwidth is to combine the rise times of the various system components and compare the result with the rise time needed for the given data rate and pulse coding scheme. The system rise time is given in terms of the data rate for non return to zero pulse code by [16]:

$$B_R\,(NRZ) = \frac{0.7}{D_t} \ , \tag{16}$$

In the same way, the device performance index (DPI) can be expressed as the following expression [18]:

$$DPI = \frac{f_m}{V_\pi}\ ,\ GHz/Volt \qquad (17)$$

IV. RESULTS AND PERFORMANCE ANALYSIS

We have investigated recent progress of $LiNbO_3$ based electrooptic modulator device in high speed photonic networks over wide range of the affecting operating parameters as shown in Table 1.

Table 1: Proposed operating parameters for our suggested electrooptic modulator device.

Operating parameter	Symbol	Value
Operating signal wavelength	λ	1.3 μm—1.55 μm
Spectral line width of the optical source	$\Delta\lambda$	0.1 nm
Ambient temperature	T	300 K ≤ T ≤ 320 K
Room temperature	T_0	300 K
Relative refractive-index change	Δn_e	0.05 ≤ Δn ≤ 0.09
Modulator length	L_m	5 cm ≤ L_m ≤ 10 cm
Speed of light	c	3 x10^{10} cm/sec
Modulator width	W	2 cm ≤ W ≤ 5 cm
Modulator thickness	d	0.2 cm ≤ d ≤ 1 cm
Gap between electrodes	g	0.1–0.35 μm
Electro-optic coefficient	r_{33}	30.8x10^{-10} cm/Volt
Applied electric field	E	2 Volt/cm
Resistivity	ρ	2.66x10^{-3} Ω.cm
Confinement factor	Γ	0.8–0.95
Modulator device capacitance	C	0.2–0.4 nF
Effective RF relative dielectric constant	ε_{eff}	17.85
Power absorption coefficient	α	0.1–0.4 dB/cm

Based on the model equations analysis, assumed set of the operating parameters, and the set of the Figs. (2–12), the following facts are assured as the following results:

i) Fig. 2 has assured that as the operating optical signal wavelength increases, this leads to decrease in device performance index at constant power absorption coefficient. As well as power absorption coefficient increases, this results in decreasing of device performance at constant operating optical signal wavelength.

ii) As shown in Fig. 3 has proved that as operating optical signal wavelength increases, this leads to increase in switching voltage at constant modulator length. As well as modulator length increases, this results in decreasing of switching voltage at constant operating optical signal wavelength.

iii) Fig. 4 has demonstrated that as gap between electrodes increases, this leads to decrease in device performance index at constant confinement factor. As well as confinement factor increases, this results of increasing of device performance index at constant gap between electrodes.

iv) Fig. 5 has indicated that as ambient temperature increases, this leads to slightly decrease in switching voltage at gap between electrodes. As well as gap between electrodes increases, this results of increasing of switching voltage at constant ambient temperature.

v) As shown in Fig. 6 has assured as both modulator length and power absorption coefficient increase, this results in decreasing of modulator transmittance.

vi) Fig. 7 has proved that as both modulator width and modulator thickness increase this leads to decrease of time constant of the modulator devices.

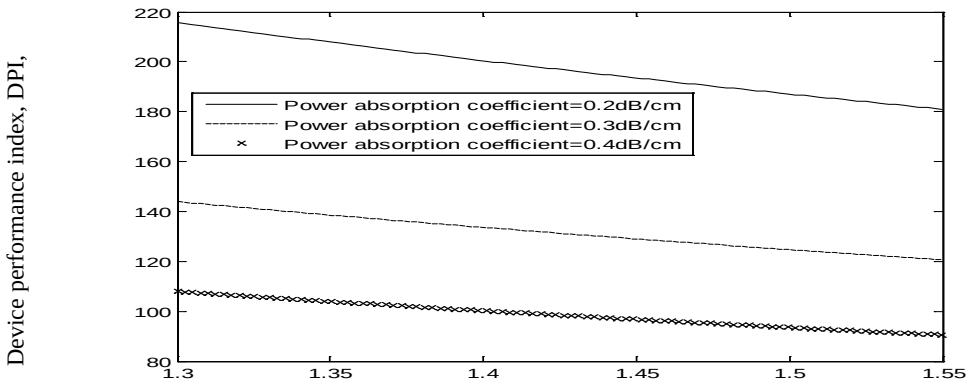

Fig. 2. Variations of the device performance index versus operating signal wavelength at the assumed set of parameters.

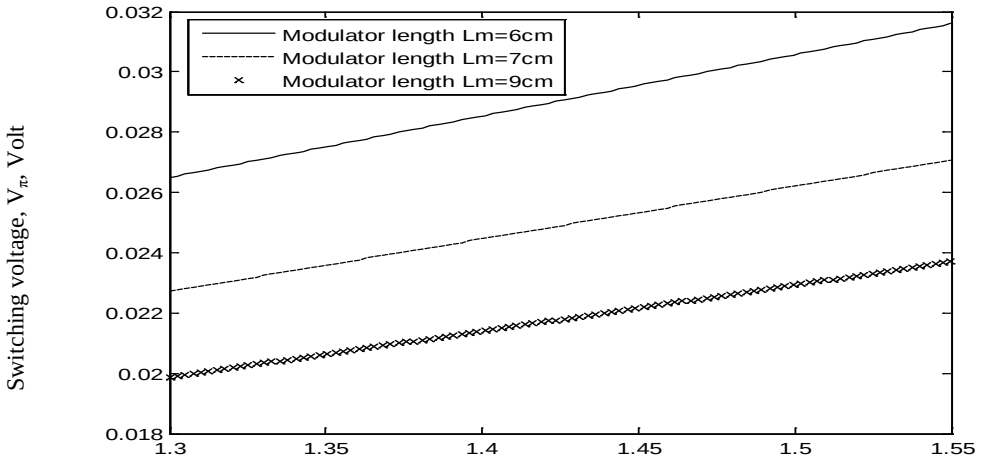

Fig. 3. Variations of the switching voltage versus operating signal wavelength at the assumed set of parameters.

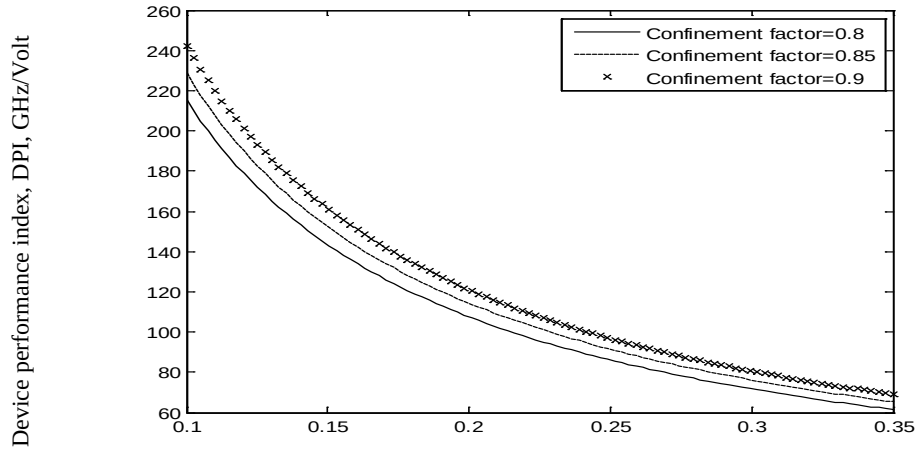

Fig. 4. Variations of the device performance index against gap between electrodes at the assumed set of parameters.

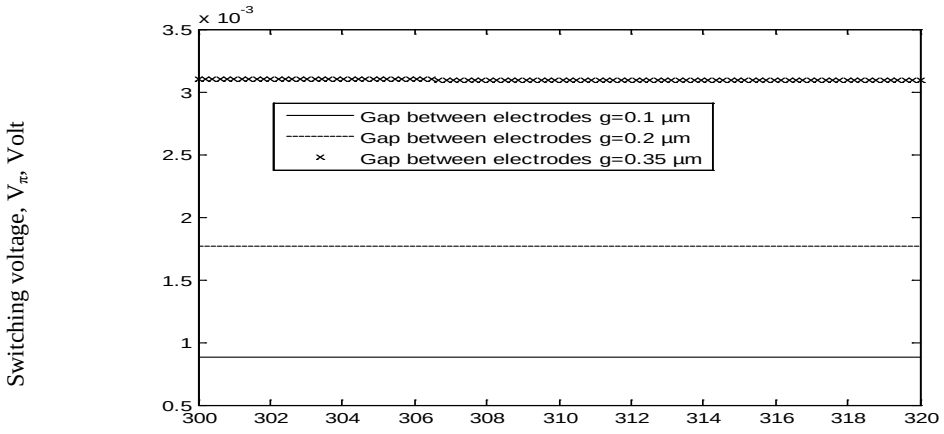

Fig. 5. Variations of the switching voltage against ambient temperature at the assumed set of parameters.

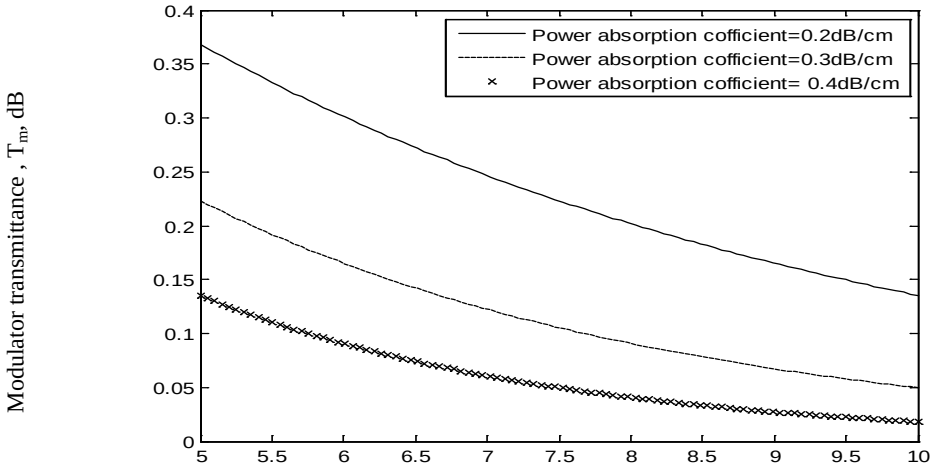

Fig. 6. Variations of the modulator transmittance against modulator length at the assumed set of parameters.

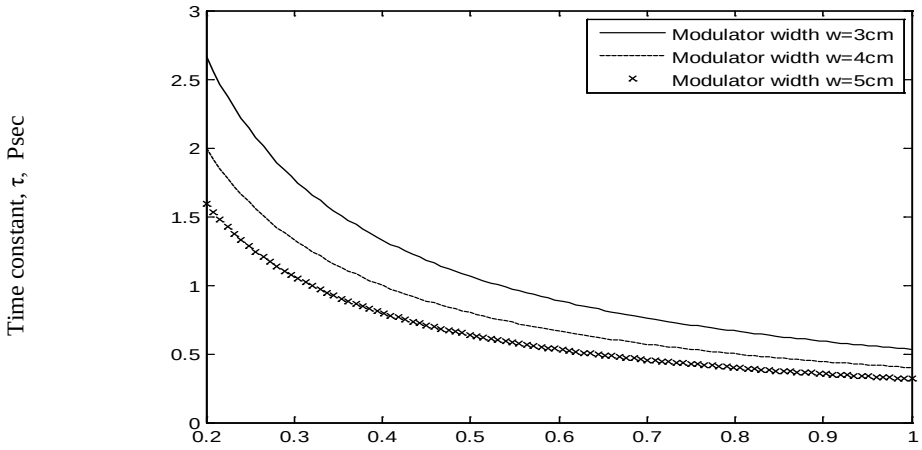

Fig. 7. Variations of modulator time constant against modulator thickness at the assumed set of parameters

.

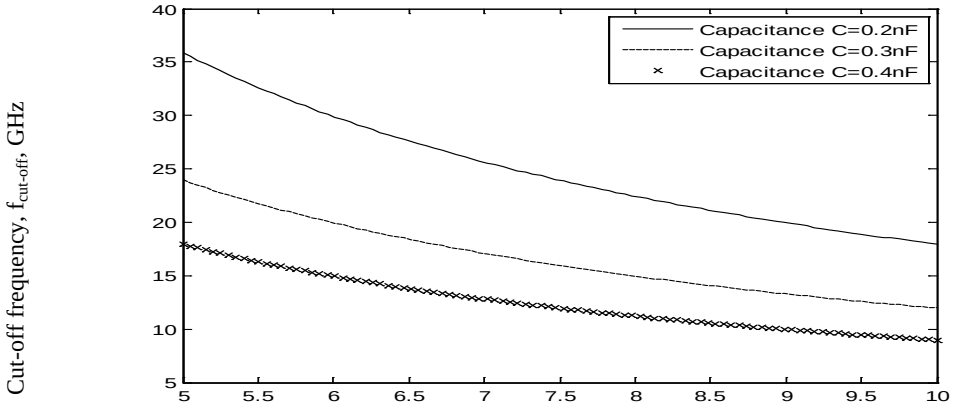

Fig. 8. Variations of cut-off frequency against modulator length at the assumed set of parameters.

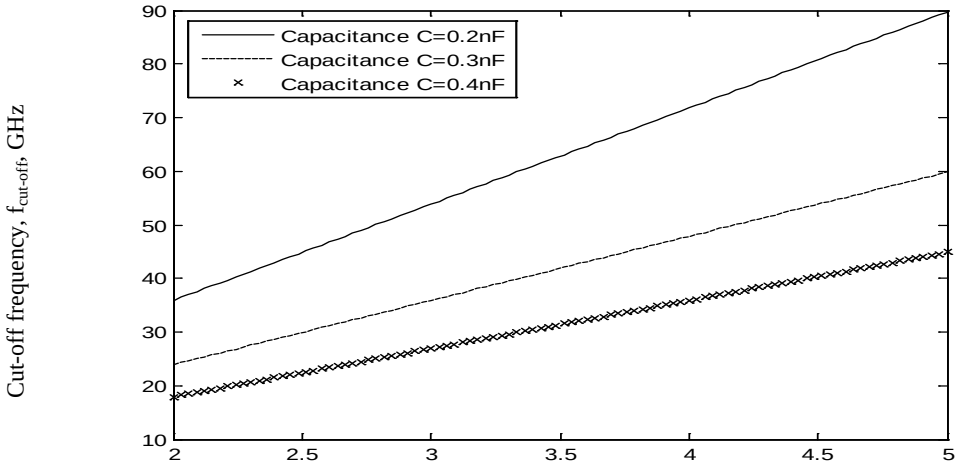

Fig. 9. Variations of cut-off frequency against modulator width at the assumed set of parameters.

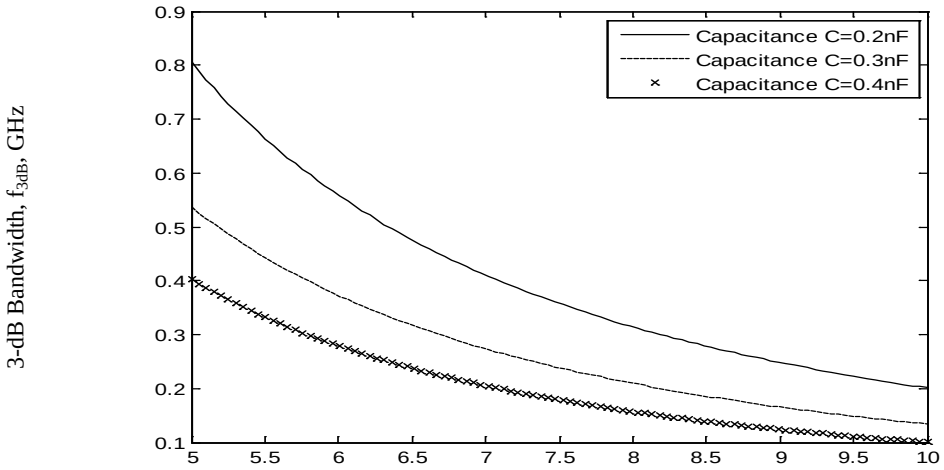

Fig. 10. Variations of 3-dB bandwidth against modulator length at the assumed set of parameters.

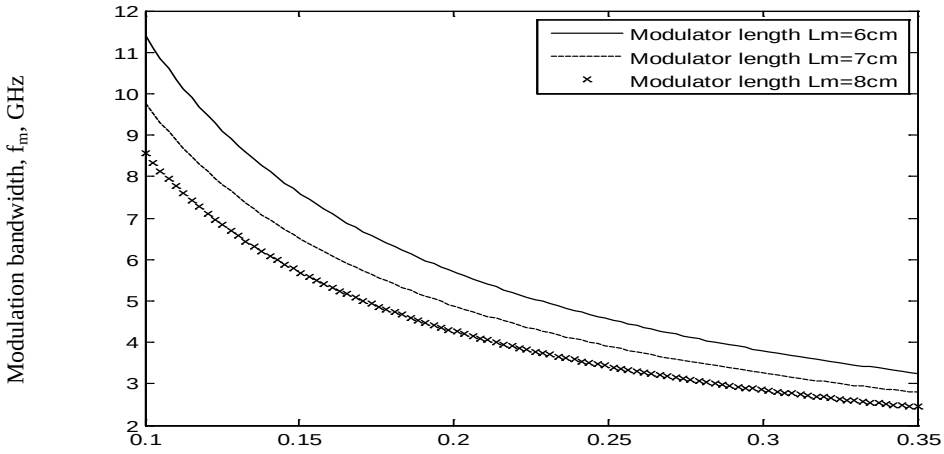

Fig. 11. Variations of modulation bandwidth against power absorption coefficient at the assumed set of parameters.

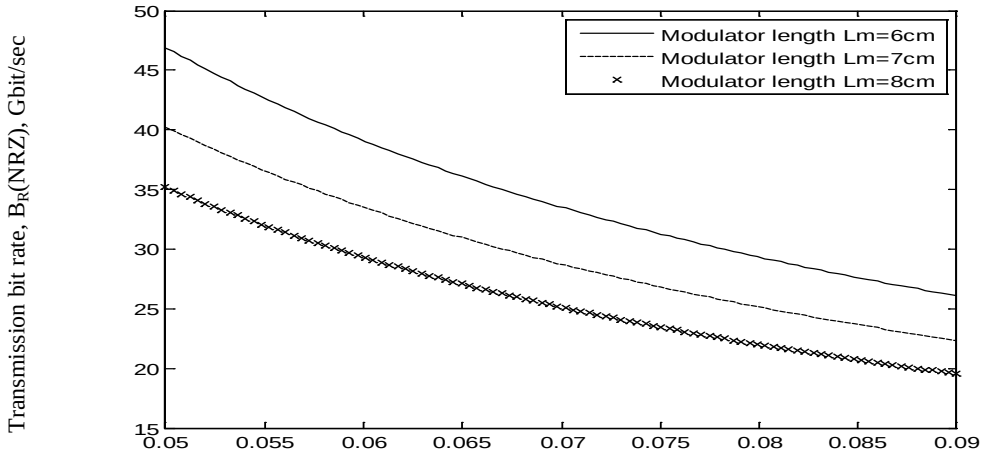

Fig. 12. Variations of transmission bit rate versus effective refractive index at the assumed set of parameters.

vii) Figs. 8 has indicated that both modulator length and modulator capacitance increase, this results in decreasing of cut-off frequency.

viii) As shown in Fig. 9 has assured that as modulator width increases and modulator capacitance decreases, this leads to increase of cut-off frequency.

ix) Fig. 10 has indicated that both modulator length and modulator capacitance increase, this results in decreasing of 3-dB bandwidth.

x) As shown in Fig. 11 has demonstrated that as both modulator length and power absorption coefficient increase, this leads to decrease of modulation bandwidth.

xi) Fig. 12 has proved that as effective relative refractive-index change and modulator length increases, this effects in decreasing in transmission bit rates of modulator devices.

V. CONCLUSIONS

In a summary, we have deeply investigated the recent progress of $LiNbO_3$ based electro-optic devices using NRZ coding to handle the modulation bandwidth, switching voltage, cut-off frequency, transmission date rate, and transmission bit rate length product. The modulator device performance parameters have been described. It is evident that of both operating optical signal wavelength and power absorption coefficient this leads to the decreased switching voltage and then the increased modulator device performance index. It is also found theoretically that the decreased gap between electrodes and the increased confinement factor this results in the increased modulator device performance index. We have observed that the decreased of both modulator length and power absorption coefficient this leads to the increased of modulator device transmittance. Moreover the increased of both modulator thickness and width this results in the decreased of time constant of the modulator device operation. As well as the decreased of both modulator capacitance and modulator length and the increased modulator width this leads to the increased cut-off frequency of the modulator devices. In the same way, we have indicated that the decreased of modulator length, modulator capacitance, power absorption coefficient, and effective relative refractive change this results in the increased of the 3-dB bandwidth, modulation bandwidth and transmission bit rates of the modulator devices.

REFERENCES

[1] M. Sugiyama, M. Doi, S. Taniguchi, T. Nakazawa, and H. Onaka, “Driver-less 40 Gb/s LiNbO3 Modulator With Sub-1 V Drive Voltage,” in Tech. Digest, Optical Fiber Communication Conference, PD FB6-2, 2002.

[2] Abd El-Naser A. Mohammed, Mohammed A. Metawe'e, Ahmed Nabih Zaki Rashed, and Mahmoud M. Eid, “Important Role of Optical Add Drop Multiplexers (OADMs) With Different Multiplexing Techniques in Optical Communication Networks,” IJCIIS International Journal of Computational Intelligence and Information Security, Vol. 1, No. 1, pp. 72-85, Jan. 2010.

[3] N. Courjal, H. Porte, A. Martinez, and J.-P. Goedgebuer, “LiNbO3 Mach-Zehnder Modulator With Chirp Adjusted by Ferroelectric Domain Inversion,” IEEE Photon. Tech. Lett., Vol. 14, No. 3, pp. 1509–1511, 2002.

[4] S. Shimotsu, S. Oikawa, T. Saitou, N. Mitsugi, , K. Kubodera, T. Kawanishi, and M. Izutsu, “Single Side Band Modulation Performance of a LiNbO3 Integrated Modulator Consisting of Four Phase Modulator Waveguides,” IEEE Photon. Tech. Lett., Vol. 13, No. 5, pp. 364–366, 2001.

[5] S. Oikawa, T. Kawanishi, K. Higuma, Y. Matsuo, and M. Izutsu, "Double Stub Structure for Resonant Type Optical Modulators Using 20-m Thick Electrode," IEEE Photon. Tech. Lett., Vol. 15, No. 2, pp. 221–223, 2003.

[6] J. Kondo, K. Aoki, A. kondo, T. Eiiri, Y. Iwata, A. Hamajima, T. Mori, Y. Mizuno, M. Imaeda, Y. Kozuka, O. Mitomi, and M. Minakata, "High Speed and Low Driving Voltage Thin Sheet X-cut LiNbO3 Modulator With Laminated Low Dielectric Constant Adhesive," IEEE Photon. Tech. Lett., Vol. 17, No. 10, pp. 2077–2079, 2005.

[7] G. L. Li, S. A. Pappert, C. K. Sun, W. S. C. Chang, and P. K. L. Yu, "Wide Bandwidth Travelling Wave InGaAsP/InP Electro Absorption Modulator for Millimeter Wave Applications," in IEEE MTT-S Int. Microwave Symp. Dig., pp. 61–64, May 2001.

[8] H. Kawanishi, Y. Yamauchi, N. Mineo, Y. Shibuya, H. Murai, K. Yamada, and H.Wada, "EAM Integrated DFB Laser Modules With More Than 40 GHz Bandwidth," IEEE Photon. Technol. Lett., Vol. 13, No. 2, pp. 954–956, 2001.

[9] Ali W. Elshaari , and Stefan F. Preble, "10 Gbit/sec Broadband Silicon Electro-optic Absorption Modulator," Optics Communications, Vol. 28, No. 3, pp. 2829–2834, Mar. 2010.

[10] H. V. Pham, and Y. Okamura, "Electrooptic Modulators with Controlled Frequency Responses by Using Nonperiodically Polarization Reversed Structure," Journal of Advances in Optoelectronics, Vol. 8 , No. 1, pp. 1-8, 2008.

[11] Abd El Naser A. Mohammed, Ahmed Nabih Zaki Rashed, Gaber E. S. M. El-Abyad, and Abd-El-fattah A. Saad "Applications of Conventional and A thermal Arrayed Waveguide Grating (AWG) Module in Active and Passive Optical Networks (PONs)," International Journal of Computer Theory and Engineering (IJCTE), Vol. 1, No. 3, pp. 290-298, Aug. 2009.

[12] T. Kawanishi, T. Sakamoto, and M. Izutsu, "High Speed Control of Lightwave Amplitude, Phase, and Frequency by use of Electrooptic Effect," IEEE Journal of Selected Topics in Quantum Electronics, Vol. 13, No. 1, pp. 79–91, 2007.

[13] H. V. Pham, H. Murata, and Y. Okamura, "Travelling Wave Electrooptic Modulators With Arbitrary Frequency Response Utilising Non Periodic Polarization Reversal," Electronics Letters, Vol. 43, No. 24, pp. 1379–1381, 2007.

[14] Abd El-Naser A. Mohammed, and Ahmed Nabih Zaki Rashed, "Comparison Performance Evolution of Different Transmission Techniques With Bi-directional Distributed Raman Gain Amplification Technique in High Capacity Optical Networks," International Journal of Physical Sciences, Vol. 5, No. 5, pp. 484-495, May 2010.

[15] M. V. Raghavendra, P. H. Prasad, "Estimation of Optical Link Length for Multi Haul Applications," International Journal of Engineering Science and Technology, Vol. 2, No.6, pp. 1485-1491, 2010.

[16] H. Tazawa and W. H. Steier, "Analysis of Ring Resonator Based Traveling Wave Modulators," IEEE Photon. Technol. Lett., Vol. 18, No. 1, pp. 211–213, 2006.

[17] H. Hu, R. Ricken, W. Sohler, and R. Wehrspohn. "Lithium Niobate Ridge Waveguides Fabricated by Wet Etching,". IEEE Photonics Technology Letters, Vol. 19, No. 6, pp. 417-419, 2007.

[18] K.Noguchi, O.Mitomi,H.Miyazawa and S.Seki,"A broadband Ti:LiNbO3 optical modulator with a ridge structure," J. Lighiwave Technol., Vol. 13, No. 3, pp.1 164-1168, 1995.